

# Chemisorption of high coverages of atomic oxygen on the Pt(111), Pd(111), and Au(111) surfaces

Cite as: Journal of Vacuum Science & Technology A **8**, 2585 (1990); <https://doi.org/10.1116/1.576675>

Submitted: 23 October 1989 . Accepted: 20 November 1989 . Published Online: 04 June 1998

Deborah Holmes Parker, and Bruce E. Koel



[View Online](#)



[Export Citation](#)

## ARTICLES YOU MAY BE INTERESTED IN

[Adsorption kinetics and isotopic equilibration of oxygen adsorbed on the Pd\(111\) surface](#)

The Journal of Chemical Physics **90**, 5787 (1989); <https://doi.org/10.1063/1.456386>

[Dependence of effective desorption kinetic parameters on surface coverage and adsorption temperature: CO on Pd\(111\)](#)

The Journal of Chemical Physics **90**, 6761 (1989); <https://doi.org/10.1063/1.456294>

[A molecular beam investigation of the catalytic oxidation of CO on Pd \(111\)](#)

The Journal of Chemical Physics **69**, 1267 (1978); <https://doi.org/10.1063/1.436666>



Advance your science and  
career as a member of

**AVS**

LEARN MORE



# Chemisorption of high coverages of atomic oxygen on the Pt(111), Pd(111), and Au(111) surfaces

Deborah Holmes Parker and Bruce E. Koel

*Department of Chemistry and Biochemistry and Cooperative Institute for Research in Environmental Sciences, University of Colorado, Boulder, Colorado 80309-0216*

(Received 23 October 1989; accepted 20 November 1989)

Studies of the interaction of oxygen with some transition metal surfaces are limited by activation barriers to adsorption and reaction of  $O_2$ . These barriers can be surmounted by using oxidants more powerful than  $O_2$  to chemisorb oxygen on these surfaces under ultrahigh vacuum (UHV) conditions, but at high "effective" pressures of  $O_2$ . We report here on the use of very reactive molecules, such as nitrogen dioxide ( $NO_2$ ) and ozone ( $O_3$ ) to study the interaction of high concentrations of oxygen atoms on the Pt(111), Pd(111), and Au(111) single crystal surfaces. Chemisorbed oxygen adatom coverages of  $\Theta_0 \leq 0.75$  monolayer (ML) on Pt(111),  $\Theta_0 \leq 1.4$  ML on Pd(111), and  $\Theta_0 \leq 0.80$  ML on Au(111) surfaces have been characterized. On the Pd(111) surface, higher concentrations ( $\Theta_0 \leq 3.1$  ML) can be formed and the initial stages of oxidation, including migration of oxygen into the subsurface region and formation of Pd oxide can be studied. This method of cleanly forming high coverages of oxygen on metal surfaces allows for new insight into the nature of oxygen-metal interactions. For example, in the case of Pt(111) and Au(111), temperature programmed desorption (TPD) can be used to determine kinetic parameters of  $O_2$  adsorption and desorption as a function of oxygen coverage and upper limits for the metal-oxygen bond strengths over a large range of oxygen coverages can be determined from the activation energy of  $O_2$  desorption. Also, the kinetics of oxidation reactions can be studied over a much larger range of oxygen coverage than previously carried out under UHV conditions on surfaces that are relatively unreactive to  $O_2$  chemisorption, such as Pt(111) and Au(111). We report preliminary results concerning transient kinetic studies of CO oxidation over Pt(111) and Au(111) surfaces.

## I. INTRODUCTION

The interaction of oxygen with transition metal surfaces has received considerable attention over the years, particularly with regard to the role of chemisorbed oxygen in oxidation reactions catalyzed on these surfaces. Fundamental studies on Pt, Pd, and Au surfaces are hampered by the small dissociative sticking probability of  $O_2$  on these surfaces. Only 0.25 monolayers (ML) of atomic oxygen can be adsorbed on Pt(111)<sup>1</sup> or Pd(111)<sup>2</sup> in ultrahigh vacuum (UHV) from exposure to  $O_2$ , and exposure of the Au(111) surface to  $O_2$  in UHV does not result in chemisorption of any measurable amount of adsorbed oxygen.<sup>3</sup> This is in contrast to other transition metals such as Rh and Ir which readily form higher saturation coverages of oxygen from  $O_2$  exposure.<sup>4,5</sup> Hence, studies of the role of adsorbed atomic oxygen in the oxidation reactions on these surfaces using techniques requiring UHV have been seriously limited by the relatively low oxygen coverages attainable under UHV conditions. This is an important consideration in applying the results obtained in UHV to catalysts operating under much higher  $O_2$  pressures and possibly much higher chemisorbed oxygen coverages.

Many methods have been used to generate high coverages of atomic oxygen on relatively unreactive surfaces. These involve electron bombardment of an  $O_2$  covered surface,<sup>6</sup> dissociation of  $O_2$  over a hot Pt or W filament so that the metal surface is exposed to O atoms,<sup>7</sup> and the use of high surface temperatures and high  $O_2$  pressures ( $> 10^{-6}$  Torr).<sup>8</sup>

These methods have distinct disadvantages. In the first two methods, the crystal must be exposed to a hot filament which can often be a source of surface contamination. Even if no deposition from the filament occurs, CO outgassed from the filament will readily titrate the surface oxygen atoms so that the maximum attainable oxygen coverage is very difficult to achieve. Using high pressures of  $O_2$  can cause problems since the concentration of  $CO_2$  and  $H_2O$  impurities often results in surface carbonate and hydroxyl formation. In this paper we illustrate another method of generating high coverages of atomic oxygen on metal surfaces from the decomposition of the highly reactive molecules  $NO_2$  and  $O_3$ . Of course, we are not the first to use this method, but we have recently made new studies which warrant reporting. We have used this method to cleanly generate oxygen coverages of  $\Theta_0 = 0.75$  ML on Pt(111) and  $\Theta_0 = 3.1$  on Pd(111) by exposing the crystals to  $NO_2$  above 400 K, and coverages of  $\Theta_0 = 0.80$  ML on Au(111) by exposing the Au surface to  $O_3$  at 300 K. These molecules are very efficient at providing oxygen to the surface. For example, we calculate that an  $O_2$  pressure of  $10^4$  atm is necessary to generate a surface oxygen concentration of  $\Theta_0 = 0.75$  ML on Pt(111) using an estimated value of 11 kcal mol<sup>-1</sup> for the activation energy of dissociative adsorption at this coverage.<sup>9</sup> In the case of Pt(111), it is known that the failure of oxygen to dissociatively chemisorb is largely due to the lack of accommodation of molecular  $O_2$  on the surface.<sup>10</sup> In contrast, the  $NO_2$  molecule has a high sticking coefficient of 0.97 at 300 K on Pt(111),<sup>11</sup> and is easily accommodated on the surface, thus providing an efficient

source of oxygen atoms. The availability of numerous weakly bound  $\text{NO}_2$  adsorption isomers has been postulated to explain the origin of this efficient accommodation.<sup>12,13</sup> It is likely that a similar situation exists for  $\text{O}_3$  since the molecules are similar in geometry and reactivity. However,  $\text{O}_3$  is exceptional in that the O–O bond strength in  $\text{O}_3(\text{g})$  is only 23 kcal/mol.

Recent work in our laboratory has reported detailed spectroscopic characterization of oxygen chemisorbed on Pt(111),<sup>9</sup> Au(111),<sup>14</sup> and Pd(111).<sup>15</sup> Briefly, on Pt(111) we found that both the work function and O (519 eV) Auger electron spectroscopy (AES) signal increased linearly with increasing surface coverage of oxygen, indicating that the oxygen is present in a similar chemical state at all coverages studied ( $\Theta_0 = 0\text{--}0.75$  ML). Ultraviolet photoelectron spectroscopy (UPS) and high-resolution electron energy-loss spectroscopy (HREELS) give evidence that all of the oxygen is present as chemisorbed atomic oxygen and low-energy electron diffraction (LEED) observations show disordering of the oxygen adlayer in one dimension at high oxygen coverages.<sup>9</sup> On the Au(111) surface, both the work function and O (519 eV) AES signal plotted versus O coverage show a change in slope near 0.50 ML, which coincides with the onset of disordering of the Au substrate.<sup>14</sup> On Pd(111), the interaction of high coverages of oxygen with the surface is quite complicated due to the formation of a Pd oxide and migration of oxygen atoms into the Pd crystal.<sup>15</sup>

In this paper, we give an overview of our studies of the interaction of high coverages of oxygen on metal surfaces, illustrating with results on Pt(111), Pd(111), and Au(111). Pt(111) shows a strong coverage dependence of the heat of adsorption of oxygen on oxygen coverage, Pd shows this variation plus oxygen penetration into subsurface sites and Au shows activated  $\text{O}_2$  adsorption even at zero coverage and disordering of the surface at high oxygen coverage. We present  $\text{O}_2$  temperature programmed desorption (TPD) data from which we have extracted the oxygen coverage dependence of the  $\text{O}_2$  desorption activation energy  $E_d$ . As an example of the interesting chemistry that can occur at high oxygen coverage, we report preliminary kinetic data for the reaction of CO with adsorbed atomic oxygen on both Pt(111) and Au(111). This method of generating high oxygen coverages allows us to follow the kinetics of the CO oxidation reaction over a range of surface oxygen coverage that is three times higher than previously reported on Pt(111). No studies have been made of the kinetics of CO oxidation on Au(111) previously.

## II. EXPERIMENTAL

The stainless steel UHV chamber used for this work is described in detail elsewhere.<sup>16</sup> The Pt(111), Pd(111), and Au(111) crystals were cleaned using standard techniques with special care taken to ensure that impurities which form refractory oxides were not present.

High purity  $\text{NO}_2$ <sup>12</sup> was used for dosing the Pt(111) and Pd(111) crystals.  $\text{NO}_2$  dosing was performed at 400 K (on Pt) and 530 K (on Pd) in order to desorb any NO or  $\text{NO}_2$ . The ozone used for dosing Au(111) was prepared in our laboratory using a commercial ozone generator and concen-

trated on a silica gel trap.<sup>14</sup> Ozone exposure was performed with the Au crystal at 300 K. A glass microcapillary array was used for dosing  $\text{NO}_2$  or  $\text{O}_3$  directly to the samples.

Absolute surface coverages of oxygen on Pd and Pt were calculated by careful comparison to the saturation oxygen coverages obtained from  $\text{O}_2$  exposure. The work of Gland<sup>7</sup> on the  $\text{O}_2/\text{Pt}(111)$  system indicates that heating a saturation coverage of  $\text{O}_2$  exposed on Pt(111) at 100 K yields  $\Theta_0 = 0.25$  ML. On the Pd(111) surface, a saturation coverage of oxygen adatoms of  $\Theta_0 = 0.25$  ML is also achieved from  $\text{O}_2$  exposure in UHV at 110 K.<sup>2,17</sup> Using these calibration points,  $\Theta_0$  was measured from the relative areas of integrated  $\text{O}_2$  TPD spectra.

Since  $\text{O}_2$  does not stick on Au(111) in UHV, the absolute oxygen coverage on Au(111) was estimated by comparing the AES peak-to-peak height ratio of O (519 eV)/Au (239 eV) with the O (519 eV)/Pt (237 eV) ratio which was obtained in the same instrument for the  $(2 \times 2)\text{-O}$  oxygen adlayer on Pt(111), which has a known oxygen coverage of  $3.8 \times 10^{14}$  atoms/cm<sup>2</sup>.<sup>1</sup> This determination is quite reliable since the kinetic energies and the relative sensitivities of the Pt (237 eV) and Au (239 eV) transitions on the clean surfaces are essentially the same.<sup>18</sup> We estimate that the saturation coverage of oxygen that we obtained with our procedure on Au(111) is  $\Theta_0 = 0.80$  ML.

To follow the transient kinetics of the CO oxidation reactions, the surface oxygen coverage was monitored during the CO titration experiments with AES. The electron beam current was adjusted to 2  $\mu\text{A}$  to avoid electron stimulated desorption or reaction: under these conditions, no observable change in oxygen signal is noticed until CO is introduced and the reaction rate was independent of the presence or absence of the electron beam.

## III. RESULTS AND DISCUSSION

### A. $\text{O}_2$ TPD from Pt(111)

Exposure of Pt(111) to  $\text{NO}_2$  at 400 K forms an atomic oxygen adlayer which desorbs as  $\text{O}_2$  to give the TPD spectra shown in Fig. 1. These spectra were generated from increasing exposures of  $\text{NO}_2$  at 400 K. Identical spectra can be obtained by annealing a saturation coverage of atomic oxygen to progressively higher temperatures prior to TPD. Figure 1 shows that four desorption peaks result from high coverages of oxygen. The high temperature state  $\beta_4$  is identical to that obtained from the saturation exposure of  $\text{O}_2$ .<sup>10,19</sup> The  $\beta_4$  peak shifts to lower temperatures with increasing  $\Theta_0$ , indicating second order kinetics. When this state reaches saturation at  $\Theta_0 = 0.25$  ML, a new state,  $\beta_3$ , appears. The  $\beta_3$  peak is invariant in temperature with increasing oxygen coverage. Above 0.40 ML two new states,  $\beta_2$  and  $\beta_1$ , appear sequentially, and also grow in with constant peak temperature. While other authors<sup>11</sup> have simply invoked pseudo-first-order kinetics, this is not easy to explain, and is not necessary, since the shape of the TPD spectra may be strongly influenced by changes in the activation energy of desorption,  $E_d$ , with coverage (*vide infra*). Previous workers have also failed to resolve the closely spaced  $\beta_2$ – $\beta_3$  "doublet". Hence, our peak numbering is different from that given by

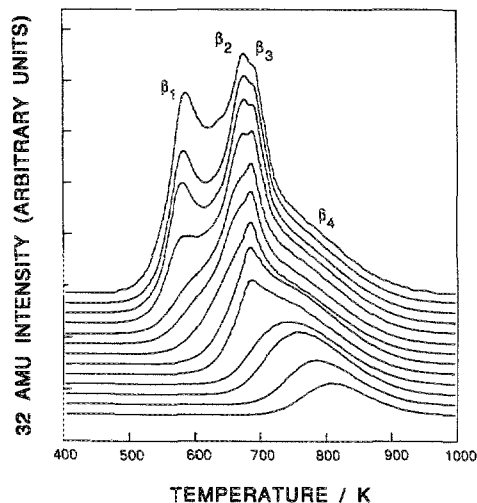


FIG. 1.  $O_2$  TPD spectra taken following varying exposures of  $NO_2$  on Pt(111) at 400 K. The spectra correspond to the following initial coverages: (a) 0.073 ML, (b) 0.093 ML, (c) 0.164 ML, (d) 0.194 ML, (e) 0.258 ML, (f) 0.291 ML, (g) 0.331 ML, (h) 0.363 ML, (i) 0.467 ML, (j) 0.534 ML, (k) 0.579 ML, (l) 0.606 ML, and (m) 0.750 ML. Taken from Ref. 5.

Segner *et al.*<sup>11</sup>: our  $\beta_4$  corresponds to the  $\beta_3$  of Segner *et al.*,<sup>11</sup> our  $\beta_2$ - $\beta_3$  "doublet" is the  $\beta_2$  state reported by Segner *et al.*<sup>10</sup> and the  $\beta_1$  states are the same in both works.

### B. $O_2$ TPD from Pd(111)

Exposure of a Pd(111) surface at 530 K to  $NO_2$  results in very high concentrations of atomic oxygen on the surface. At the highest concentrations ( $\Theta_0 \geq 1.4$  ML), two low-temperature desorption states (which could not be obtained from  $O_2$  exposure in UHV) were never observed to saturate for any exposure of  $NO_2$ . Oxygen concentrations greater than 3 ML were observed (calculated from integrated  $O_2$  TPD areas). Figure 2 shows  $O_2$  desorption traces resulting from  $0.61 \leq \Theta_0 \leq 1.2$  ML. Curves (a) and (b) have leading edges which overlay, but the peak maxima cross through the leading edges of curves (c) and (d) obtained for higher coverages. AES, x-ray photoelectron spectroscopy (XPS), and HREELS data indicate that oxygen is present at 100 K as chemisorbed atomic oxygen for coverages up to  $\Theta_0 = 1.4$  ML. At higher coverages ( $\Theta_0 \geq 1.4$  ML), oxygen migrates to subsurface sites and oxide formation occurs at or near the surface. The TPD spectra shown in Fig. 2 are governed by complex desorption kinetics, since  $O_2$  desorption is a competitive process between subsurface diffusion and oxygen adatom recombination at the surface for  $0.75 \leq \Theta_0 \leq 1.4$  ML.

### C. O/Au(111) TPD

Exposure of Au(111) to  $O_3$  at 300 K forms an atomic oxygen adlayer which desorbs to produce the  $O_2$  TPD spectra shown in Fig. 3. These spectra were generated from increasing exposure to  $O_3$  at 300 K. Exposures to  $O_2$  at 300 K resulted in no detectable  $O_2$  TPD peak. Oxygen coverages were determined by relative integrated  $O_2$  TPD areas, with the saturation coverage calibrated by AES (*vide supra*). Figure 3 shows that the peak maximum and peak shape both

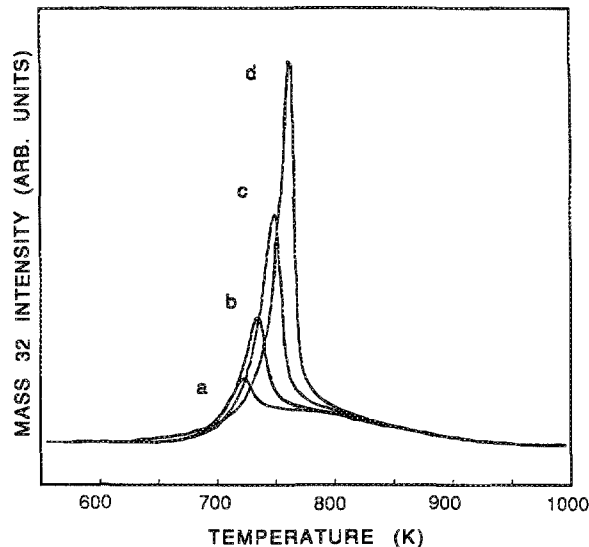


FIG. 2.  $O_2$  TPD spectra following increasing exposures to  $NO_2$  on Pd(111) at 530 K. The initial oxygen coverages are (a) 0.61 ML, (b) 0.76 ML, (c) 1.0 ML, (d) 1.2 ML. Taken from Ref. 14.

change with coverage. At low coverages ( $\Theta_0 \leq 0.07$  ML), the peak maximum shifts to higher temperatures with increasing coverage, implying an increasing activation energy of desorption. At higher oxygen coverages ( $\Theta_0 > 0.15$  ML) the peak maximum is only slightly dependent on coverage and has an asymmetric shape indicative of first order desorption kinetics. This is surprising since one would expect  $O_2$  desorption to follow second order kinetics.

### D. Activation energy of $O_2$ desorption

We have used a variety of methods to analyze the coverage dependence of the activation energy of  $O_2$  desorption using the TPD data shown in Figs. 1 and 2. These methods are described in detail in several papers.<sup>9,14,20,21</sup> The results of analyses using these methods are shown in Figs. 4 and 5 for Pt(111) and Au(111), respectively.

Figure 4 shows  $E_d$  versus oxygen coverage as determined from the TPD data in Fig. 1. It can be seen that  $E_d$  is not constant, and is a very strong function of coverage. For the range  $\Theta_0 = 0$  to 0.25 ML, a decrease occurs in  $E_d$  from 51 kcal/mol in the limit of zero coverage to 43 kcal/mol at  $\Theta_0 = 0.25$  ML. This is in excellent agreement with Campbell *et al.*<sup>10</sup> who report a variation of 51 to 41 kcal/mol over the same coverage range. We find that  $E_d$  decreases strongly with increasing oxygen coverage above  $\Theta_0 = 0.25$  ML, so that  $E_d = 29$  kcal/mol at  $\Theta_0 = 0.32$  ML. The desorption activation energy decreases only slightly to 28 kcal/mol at  $\Theta_0 = 0.40$  ML, but then rises sharply to 38 kcal/mol at  $\Theta_0 = 0.42$  ML and falls sharply to 28 kcal/mol at  $\Theta_0 = 0.45$  ML. A slight rise in  $E_d$  occurs above  $\Theta_0 = 0.50$  ML before  $E_d$  falls linearly with oxygen coverage to 28 kcal/mol at  $\Theta_0 = 0.75$  ML. The complicated behavior of the activation

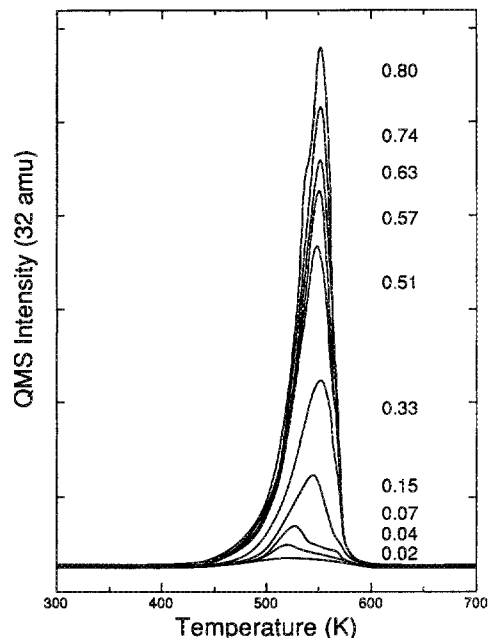


FIG. 3.  $O_2$  TPD spectra following increasing exposure to  $O_2$  on Au(111) at 300 K. The initial oxygen coverages are (a) 0.02 ML, (b) 0.04 ML, (c) 0.07 ML, (d) 0.15 ML, (e) 0.33 ML, (e) 0.51 ML, (f) 0.51 ML, (g) 0.57 ML, (h) 0.63 ML, (i) 0.74 ML, and (j) 0.80 ML. Taken from Ref. 13.

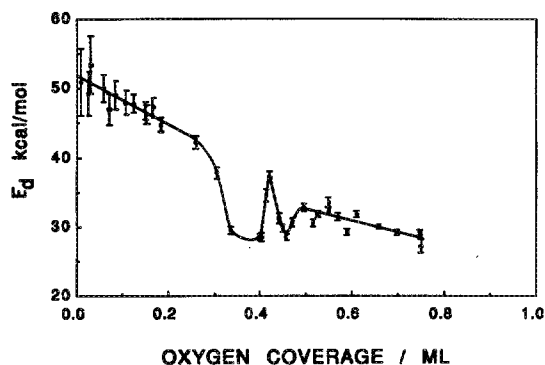


FIG. 4. Plot of the activation energy for  $O_2$  desorption  $E_d$  vs oxygen coverage on Pt(111). Taken from Ref. 5.

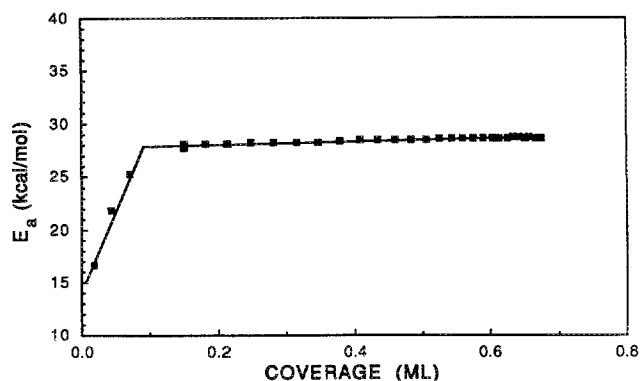


FIG. 5. Summary of  $O_2$  TPD data analysis showing the variation of the activation energy for  $O_2$  desorption from Au(111) as a function of oxygen coverage. Taken from Ref. 13.

energy of desorption is due to changes in the binding energy of atomic oxygen and the activation barrier to  $O_2$  adsorption.

Oxygen TPD spectra from the Au(111) surface are surprising. The spectra have the appearance of first order desorption kinetics which is unexpected for recombination of atomically adsorbed oxygen species. Analysis of the TPD data using plots of  $\ln(\text{rate}) - n \ln(\Theta)$  to determine the reaction order  $n$ , gives linear plots for  $n = 1$ , in the region of the peak maximum,<sup>20</sup> indicating that the desorption curves are well described by first-order kinetics. Figure 5 summarizes the results of our analysis of the coverage dependence of  $E_d$  for  $O_2$  desorption from Au(111). There is rapid increase in  $E_d$  with increasing coverage from 16.0 kcal/mol near  $\Theta_0 = 0$  ML to 28.0 kcal/mol at  $\Theta_0 = 0.07$  ML.  $E_d$  then shows a very slight increase to 28.8 kcal/mol near saturation coverages. The results presented in Fig. 5 correlate well with the empirical observation that the temperature of the desorption peak maximum increases significantly with coverage at the three lowest coverages studied and then shifts only very slightly to higher temperatures with higher coverages. The rapid rise at low coverage occurs in a regime where the clean Au(111) reconstruction is lifted and where there are likely to be some effects due to defect sites.

We know that  $O_2$  dissociative chemisorption is an activated process on Au(111) and the  $E_d$  measured from TPD reflects the sum of the adsorption energy ( $\Delta E_{\text{ads}}$ ) and the activation energy for dissociation ( $E_a$ ). An explanation for the rapid rise in  $E_d$  at low  $\Theta_0$  ( $< 0.07$  ML) is that initially defect sites are populated which have much lower  $E_a$  and consequently lower  $E_d$ . The small rise in  $E_d$  over the range  $\Theta_0 = 0.07$ – $0.80$  ML could be due to inductive electronic effects whereby adsorbed oxygen withdraws charge from Au surface atoms and increases the subsequent interaction between  $Au^{\delta+}$  and  $O^{\delta-}$ . The first order desorption kinetics of  $O_2$  are difficult to explain, but could be due to reconstruction of the Au(111) surface being the rate-limiting step for  $O_2$  desorption. Long-range disordering of the surface was observed using LEED at higher oxygen coverages.

Since  $O_2$  will not dissociatively chemisorb on Pt(111) above  $\Theta_0 = 0.25$  ML, this implies the existence of an energetic barrier to  $O_2$  adsorption at this coverage. By populating the surface to a coverage greater than 0.25 ML, we can indirectly probe the adsorption barrier height, since the oxygen desorbs as  $O_2$  molecules. However, we cannot measure the barrier height directly from TPD experiments. We can only measure the desorption activation energy  $E_d$  which is the sum of the heat of dissociation adsorption  $E_{\text{ads}}$  and the activation barrier to adsorption,  $E_a$ . The same argument holds true for the Au(111) system which has a barrier to  $O_2$  adsorption for the clean surface. This method of generating high coverages of oxygen using reactive molecules holds promise for accurately determining metal–oxygen bond strengths if future experiments were to measure these barrier heights. For now, crudely estimating the height of the barriers has allowed us only to make estimations of the upper limits on the metal–oxygen bond strengths. We have determined that the upper limit on the Pt–O bond strength is 65 kcal/mol at  $\Theta_0 = 0.75$  ML and the upper limit on the Au–O bond strength is 74 kcal/mol at  $\Theta_0 = 0.80$  ML. These bond

strengths can be better defined once accurate adsorption energies are known.

### E. Reactivity of high coverages of atomic oxygen

We have performed transient kinetic studies of the reactivity of high coverages of atomically adsorbed oxygen on Pt(111) and Au(111) with CO. Studies of the mechanism of catalytic reactions can be greatly simplified by using transient techniques in which one reactant is first preadsorbed onto the surface and then reacted away by the introduction of the second reactant. In this manner, kinetic effects of the adsorption of one reactant can be separated from those of the surface reaction.

A typical titration transient experiment consisted of pre-dosing the crystal with NO<sub>2</sub> (for Pt) or O<sub>3</sub> (for Au) to obtain the desired atomic oxygen coverage, followed by heating the crystal to the desired reaction temperature. A pressure jump of CO was then introduced. The O (KVV) AES signal was monitored as a function of time for the duration of the reaction to yield  $\Theta_0(t)$ . The oxygen AES signal has been shown previously to be proportional to  $\Theta_0$  on both Pt(111)<sup>9</sup> and Au(111).<sup>14</sup> Numerical differentiation of this signal was used to calculate rate ( $d\Theta_0/dt$ ) versus time. Rate versus oxygen coverage could be calculated also, since the oxygen AES signal can be used to deduce  $\Theta_0$  at any time.

#### 1. CO+O/Pt(111)

Figure 6(a) shows the measured data [O (KVV) signal versus time] obtained for the conditions  $P_{\text{CO}} = 2 \times 10^{-9}$  Torr and a sample temperature of 500 K. This curve shows that the oxygen signal decays over a period of 950 s to a constant value where  $\Theta_0 = 0$ . The derivative of this curve yields the reaction rate as a function of time, which is shown in Fig. 6(b). This figure clearly shows that the rate increases as a function of time, reaching a maximum value at approximately 850 s. At approximately 950 s the rate rapidly decreases and then goes to zero. These results are in contrast to studies using an initial oxygen coverage of  $\Theta_0 = 0.25$  ML in which the rate reached a maximum quickly and then decreased.<sup>22</sup>

We also show in Fig. 6(c), the CO oxidation rate at 500 K plotted as a function of  $\Theta_0$ . At low  $\Theta_0$  ( $< 0.1$  ML), the CO<sub>2</sub> production rate is directly proportional to  $\Theta_0$ . The rate is nearly constant, independent of  $\Theta_0$  for  $0.1 \leq \Theta_0 \leq 0.25$  ML. This suggests that an adsorbed precursor state of CO exists which is important to the kinetics. Work by Campbell *et al.*<sup>23</sup> for coverages up to 0.25 ML also suggests such a precursor state. For coverages larger than  $\Theta_0 = 0.25$  ML, the rate decreases with increasing oxygen coverage. One explanation is that the CO<sub>2</sub> formation rate is proportional to the sticking coefficient of CO,  $S_{\text{CO}}$  which has a  $(1 - \Theta_0)$  functional form. This  $\Theta_0$  dependence of  $S_{\text{CO}}$  has not been seen on Pt(111) previously. We are presently analyzing transient kinetic data taken at a variety of temperatures and pressures in order to obtain values for the activation energy and reaction order in  $P_{\text{CO}}$  in order to provide a better understanding of the mechanism of the CO oxidation reaction at these high oxygen coverages.

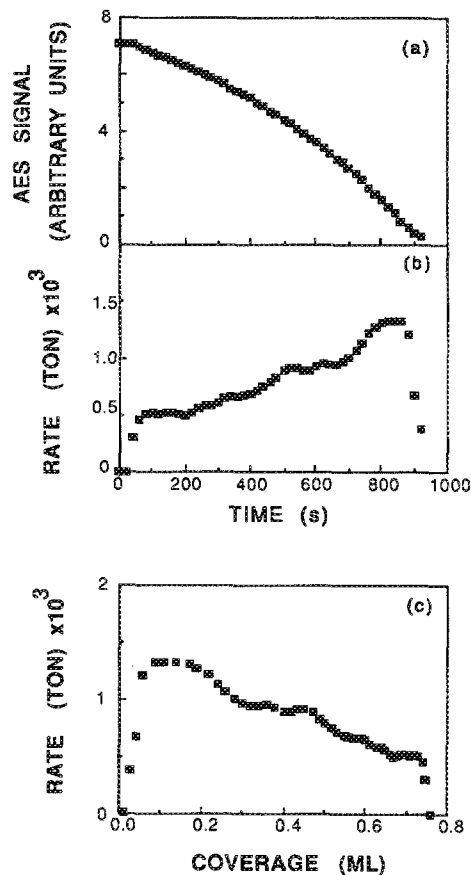


FIG. 6. Transient kinetic results for CO oxidation on Pt(111). The experimental conditions are  $T = 500$  K and  $P_{\text{CO}} = 2 \times 10^{-9}$  Torr. Panel (a) shows the raw data for the O (KVV) AES signal as a function of time. Panel (b) shows the CO oxidation rate as a function of time. Panel (c) shows the reaction rate as a function of atomic oxygen coverage,  $\Theta_0$ .

#### 2. CO+O/Au(111)

We have performed transient kinetic experiments, similar to those described above, for CO oxidation on the O-covered Au(111) surface. Figure 7 shows the results of a typical transient kinetic experiment with  $P_{\text{CO}} = 5 \times 10^{-8}$  Torr and  $T = 300$  K. Panel (a) shows the AES signal intensity as a function of time showing the decrease of the oxygen concentration over a period of 1375 s. Panel (b) shows the derivative of the data in panel (a), showing the reaction rate as a function of time. The CO oxidation rate decreases with time as the oxygen coverage decreases. Panel (c) shows this explicitly by plotting the CO oxidation rate as a function of oxygen coverage. The reaction rate is linear with oxygen coverage and increases steadily over the entire course of the reaction, indicating that the reaction is first order in oxygen coverage up to  $\Theta_0 = 0.80$  ML! At present we are analyzing additional data for a range of experimental conditions in an attempt to determine the mechanism and energetics of this reaction. Preliminary results show that the reaction rate increases at lower surface temperatures reaction has an apparent negative activation energy. This negative apparent activation energy is the energy difference between the Langmuir-Hinshelwood (LH) activation energy of the O(a) + CO(a) reaction,  $E_{\text{LH}}$ , and the activation energy for de-

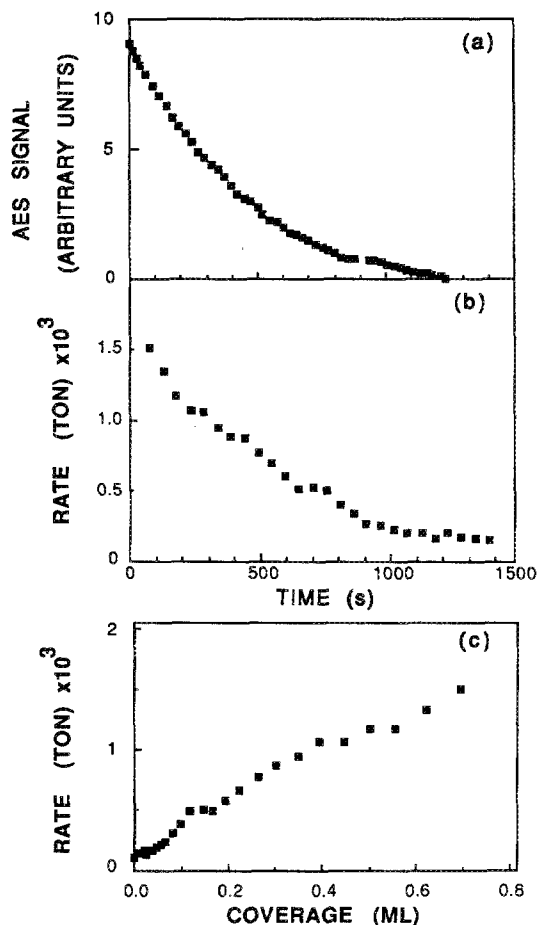


FIG. 7. Transient kinetic results for CO oxidation on Au(111). The experimental conditions are  $T = 300$  K and  $P_{\text{CO}} = 5 \times 10^{-8}$  Torr. Panel (a) shows the raw data for the O(KVV) AES signal as a function of time. Panel (b) shows the CO oxidation rate as a function of time. Panel (c) shows the reaction rate as a function of atomic oxygen coverage,  $\Theta_0$ .

sorption of CO,  $E_d$ . Since  $E_d^{(\text{CO})}$  is so small [CO will not adsorb on Au(111) at 100 K], the surface reaction barrier,  $E_{\text{LH}}$ , is very small. Still, the reaction mechanism is via a LH pathway rather than via an Eley-Rideal pathway.

#### IV. CONCLUSIONS

The use of reactive molecules such as  $\text{NO}_2$  and  $\text{O}_3$  to generate high coverages of atomic oxygen on transition metals has opened up several new avenues of research on the interactions of atomic oxygen with these surfaces. We have characterized the interaction of oxygen with Pt(111), Pd(111), and Au(111). We have found that high concentrations of atomic oxygen can be achieved on these surfaces:  $\Theta_0 = 0.75$  ML on Pt(111),  $\Theta_0 = 3.1$  ML on Pd(111), and  $\Theta_0 = 0.80$

ML on Au(111). As an example of the interesting chemistry that is found, we have used TPD to determine that the activation energy for desorption of  $\text{O}_2$  from Pt(111) and Au(111) is a strong function of oxygen atom coverage and we have used transient kinetic methods to determine that the CO oxidation rate is also a strong function of oxygen atom coverage on both Pt(111) and Au(111).

The capability to form these high coverages of oxygen on relatively unreactive transition metal surfaces should allow us to study the kinetics of oxidation reactions over a much wider range of oxygen coverages than previously available.

#### ACKNOWLEDGMENTS

This work was supported in part by the U.S. Department of Energy, Office of Basic Energy Sciences, Chemical Sciences Division. Acknowledgment is also made to the donors of the Petroleum Research Fund administered by the American Chemical Society for partial support of this work. DHP also thanks the Exxon Educational Foundation for providing an Exxon Fellowship. We also would like to thank our co-workers Barbara Banse, Mike Bartram, Dave Wickham, and Mark Jones for their help in various aspects of these experiments.

<sup>1</sup>P. R. Norton, J. A. Davies, and T. E. Jackman, *Surf. Sci.* **122**, L593 (1982).

<sup>2</sup>H. Conrad, G. Ertl, J. Kuppers, and E. Latta, *Surf. Sci.* **65**, 245 (1977).

<sup>3</sup>J. J. Pireaux, M. Chtaib, J. P. Delrue, P. A. Thiry, M. Liehr, and R. Caudano, *Surf. Sci.* **141**, 211 (1984).

<sup>4</sup>T. W. Root, L.D. Schmidt, and G. B. Fisher, *Surf. Sci.* **134**, 30 (1983).

<sup>5</sup>Ts. S. Marinova and K. L. Kostov, *Surf. Sci.* **185**, 203 (1987).

<sup>6</sup>H. Steininger, S. Lehwald, and H. Ibach, *Surf. Sci.* **123**, 1 (1982).

<sup>7</sup>J. L. Gland, *Surf. Sci.* **93**, 487 (1980).

<sup>8</sup>G. N. Derry and P. N. Ross, *Surf. Sci.* **140**, 165 (1984).

<sup>9</sup>D. H. Parker, M. E. Bartram, and B. E. Koel, *Surf. Sci.* **271**, 489 (1989).

<sup>10</sup>C. T. Campbell, G. Ertl, H. Kuipers, and J. Segner, *Surf. Sci.* **107**, 220 (1981).

<sup>11</sup>J. Segner, W. Vielhaber, and G. Ertl, *Isr. J. Chem.* **22**, 375 (1982).

<sup>12</sup>M. E. Bartram, R. G. Windham, and B. E. Koel, *Surf. Sci.* **184**, 57 (1987).

<sup>13</sup>M. E. Bartram, R. G. Windham, and B. E. Koel, *Langmuir* (in press).

<sup>14</sup>D. H. Parker and B. E. Koel, *Surf. Sci.* (submitted).

<sup>15</sup>B. Banse and B. Koel, *Surf. Sci.* (submitted).

<sup>16</sup>R. G. Windham, M. E. Bartram, and B. E. Koel, *J. Phys. Chem.* **92**, 2862 (1988).

<sup>17</sup>T. Matsushima, *Surf. Sci.* **157**, 297 (1985).

<sup>18</sup>*Handbook of Auger Electron Spectroscopy*, 2nd ed. (Physical Electronics, Eden Prairie, MN, 1976).

<sup>19</sup>J. L. Gland, B. A. Sexton, and G. B. Fisher, *Surf. Sci.* **95**, 587 (1980).

<sup>20</sup>D. H. Parker, M. E. Jones, and B. E. Koel, *Surf. Sci.* (submitted).

<sup>21</sup>M. E. Jones, D. H. Parker, and B. E. Koel, *Surf. Sci.* (submitted).

<sup>22</sup>F.-H. Tseng and J. M. White, *Int. J. Chem. Kinet.* **7**, 417 (1980).

<sup>23</sup>C. T. Campbell, G. Ertl, H. Kuipers, and J. Segner, *J. Chem. Phys.* **73**, 5862 (1980).